

Lagrangian Formalism Based Human Confidence Modelling During Decision Making

Arnab Rakshit, Uddhav Sen

Abstract—The paper proposes a Collaborative Brain Computer Interface framework for multiple opinion fusion using a novel metric of human confidence. The framework is primarily effective in the defense sector for detecting target object/s from real time satellite images. Proposed BCI system uses P300 brain response and eyeball position of the experts to automatically detect the target object and localize it in the image frame respectively. Individual decision of each expert is captured using EEG signal which is fed to a decision fusion algorithm to generate the final decision. The paper derives a novel metric of human confidence using Lagrangian action formalism and uses it to verify the decisions taken by the individual experts. The work also provides a mathematical justification of considering Lagrangian action as a valid measure of human confidence. Inclusion of such a certainty measure has significantly increased the overall correctness (GM) of the system and adjusted F-measure by a margin of 5.39% and 5.20% respectively on average. Reliability of the system (kappa score) is also increased by 8.0%. The system also shows a robust behaviour under faulty conditions where experiment shows that system is able to maintain the average overall accuracy of 84.98% with average inter (kappa score) and intra-group (ICC1) reliability value of 0.84 and 0.69 respectively even when the majority of the group members fail to deliver. Result of individual and group wise performance is presented at the end of study and compared with other standard state-of-the-art algorithms.

Impact Statement—The current paper aims to construct a novel class of human Confidence(certainty) measures for a Brain-Computer Interface(BCI) based Collaborative Decision fusion algorithm/setup inspired by the Lagrangian Formulation of Analytical Mechanics in abstract Information Space. Contrary to the existing method of adopting a heuristic measure of human confidence arising from reaction time and neural features, the present paper provides a closed framework of opinion fusion. Such a general framework would enable any Collaborative BCI setup to precisely evaluate the confidence of the members directly from their brain response during the decision making and to include the same in the final decision fusion process. The paper derives the interconnection between Information Entropy and Lagrangian formulation and obtains a stationary Action which helps in constructing a novel measure of confidence with greater precision as it is more fundamental and it represents a more accurate description of the Information trajectory for cognitive-based fusion models. The paper also justifies treating Information content as a generalized coordinate in the Lagrangian formulation which implies that it can be used on stochastic multi-body systems. The inclusion of such a certainty measure has significantly increased the overall correctness and reliability of the BCI-based collaborative decision-making process. The system also shows robust behavior under faulty conditions when the majority of the group members fail to deliver which might otherwise turn out to be fatal in real-time Defense-related operations.

Index Terms—EEG, EOG, BCI, Certainty, SVM, RBF, Satellite Image, Surveillance, Lagrangian Mechanics, Entropy, Information Space.

I. INTRODUCTION

Developed nations use real time satellite images for border surveillance. Satellite and thermal imagery provides certain benefits over cloud cover, fog and smoke. As high resolution imagery is not preferred for real time processing due to the requirement of high computational resources; the low resolution, small object to background ratio and lack of detailed images makes automated object recognition a great challenge [1]. Suspicious object detection and decision making in military systems is still considered a complex problem in spite of great progress in automated object recognition processes in recent years. Moreover various object recognition algorithms may be well suited for general purpose object detection schemes but fall short behind in military systems where adversarial attacks from the enemy side always try to fool an AI engine in the hopes of avoiding detection [2][3]. The military decision making process includes factors like the strength of own forces, estimated force and intentions of enemy, weather- and terrain conditions, behaviour of the population, communications, etc. Such complex decision making task is challenging for any AI model. Hence a human assisted decision making scheme is necessary to be implemented where a target object is determined by fusing the decision of multiple experts. The inclusion of multiple experts reduce the error which might come from a single human observer(wisdom of crowd), and enhances the robustness of the decision [4][5]. Such collaborations are found to be effective specifically in military decision making [6][7]. The two major drawbacks of the collaborative decision making process is that traditional verbal communication or opinion sharing based group decision fusion technique imposes an obstacle to the optimal decision making due to several factors [8][9] and the lack of closed solution to measure the confidence of an expert during the decision making process.

Here,we propose a novel collaborative technique of target object detection using Brain Computer Interface [10] framework which includes a novel measure of cognitive confidence of the human observers as a prime factor of decision making. Decision fusion using BCI provides a superior performance over non-BCI technique in terms of accuracy and speed [11][12]. The paper uses a direct communication channel between brain and computer [13], where the cognitive activity of each human observer is captured in terms of Electroencephalographic (EEG) signal that is directly processed by the computer to obtain the final decision.

An oddball brain signal P300 is used to capture the human intention about the target object. Infrequent and odd stimuli elicit P300 brain pattern after approximately 300 ms of onset

of visual stimulus [14]. Exact location of the target object is found by using Electrooculogram (EOG) signal which captures the eye movement of the human observer in terms of potential variation. A suitable calibration between eye ball position and image co-ordinates provides the object location in the image frame [15]. Object location is recorded at the time of occurrence of P300 along with the certainty with which the subject takes the decision. Individual decision of each expert is fed to a decision fusion algorithm to generate the final decision. A particular object is marked as important only when the output from the group decision classifier is found to be true.

The major contribution of the present paper is the derivation of novel analytic measure of human confidence from EEG signal using Lagrangian action formalism. This paper uses a framework which takes Information content as the state variable in the Lagrangian formalism and develops a unique measure of confidence for individual participating subject. Dual correspondence between physical space and abstract Information content space is established here. Stochastic least action path arises from principle of maximum physical entropy which becomes Shannon Entropy under the optimal probability distribution implying a duality between the most stable stochastic system evolution(least action) from maximum physical entropy and least certain path in Information space. The least certain path contains maximum unknown Information content and hence exploiting such a path will give maximum non correlated knowledge about the system. The paper also provides a considerable extension of work [16][17] which was primarily targeted to show the equivalence between principle of maximum entropy and stochastic stationary action principle. There exists few literature which utilises maximum entropy principle to optimise path planning in disturbed environments[18][19] but the interconnection between Information entropy and Lagrangian formalism has not been extensively explored. Although there has been some developments like Balasuriya *et al.*[20] which discuss about applications of Lagrangian coherent structures in clustering problems and Branicki *et al.* in [21] that proposes trajectory based predictions for Eulerian vector fields but neither of the above work exploits the link between optimal Information flow and the most stable stochastic evolution. The current paper utilises the equivalence between the most fundamental laws of physics to optimally derive the most evident path evolution in dual physical and Information space for random processes. Furthermore, it validates the claim of using Information space based Lagrangian Action as a confidence measure for the collaborative decision fusion process. As a corollary, the paper justifies treating information content as generalised co-ordinate in the Lagrangian under the abstract mass of system opposing acceleration and proves that variational formalism can be used on stochastic multi-body systems.

We employ a distance metric approach to incorporate the measure of confidence and subjective accuracy in the group classification algorithm. Contrary to the method of adopting a heuristic measure [22][23][12]arising from reaction time and neural features, the present paper provides a general framework of opinion fusion using the analytical solution. The

neural features arising from the P300 signal are subsets of the total Information Space pool considered here. The paper also re-structures the framework of c-BCI using a two fold cost-effective strategy. First the paper uses Electroocculogram (EOG) instead of any eye tracking device, as the EOG device is a low budget instrument and working with EOG requires less computational resources. The number of EEG electrodes are also reduced to three, which makes the system feasible for real time operations and more suitable to be implemented as a standalone system.

Rest of the paper is as follows. Related works are presented in Section II, Section III elaborates the proposed method in detail and Section IV describes the process of P300 detection. Details of EOG and object localisation is explained in section V. Section VI contains the theoretical framework and derivation of the certainty measure. The theoretical justification of the proposed certainty measure is provided in Section VII. Collaborative framework for multiple decision fusion is given in section VIII. Section IX contains the experimental protocol and results. Section X provides the statistical validation of the proposed collaborative classifier. Concluding remarks and major findings of the study are added in Section XI.

II. RELATED WORKS

Literature shows the hybrid use of EEG and EOG signal for various BCI based scheme [24] [25]. EEG and EOG based hybrid BCI(hBCI) has also been successfully used in target detection [26][27] but the works rely on single user opinion at a time. Such an approach is not suitable in defense sectors where multiple opinion is encouraged before arriving at any decision as it eliminates any bias an officer might have from his/her past experience [28]. Multiple opinion fusion in military decision making also provides a superior performance over single user opinion[6][7] .

Wang *et al.*[29] invoked the idea of c-BCI for predicting motor movement direction and found a significant increase in classification accuracy over single user performance. Eckstein *et al.*[30] presented a collaborative approach to find out the efficacy of multi brain computing. The work also advances the understanding about the neural basis of collective wisdom. Another multi-brain fusion technique was established by Stoica *et al.* [31], which showed the efficacy of multi-brain fusion to integrate more information than any other verbal and non-verbal means. Fernandez *et al.* [32] have given a novel c-BCI paradigm to automatically classify target and non-target images using rapid serial visual presentation (RSVP). Another work on c-BCI demonstrates the use of Visual Evoked Potential based online classification of target and non-target images [33]. Yuan *et al.* [34] showed that collaborative BCI can accelerate the decision making process and also increase the prediction rate of the decision in real time. Optimal combination of subjects and EEG electrodes per subject can play a crucial role in determining the correct final decision, such factors of c-BCI are thoroughly analysed in the work of Cecotti *et al.* [35]. c-BCI is also used for rapid face recognition task based on single trial response and it is shown that collaborative approach outperforms the single human based approach by a significant margin [36]. From 2016

to 2019, few consecutive studies have combined BCI with human behavioral response. They have mainly relied on RSVP protocol of image representation and on the VEP response revealed by EEG to detect the target image in complex natural environment [37][22][38][12][39][40]. The application of those works includes movement planning task, detection of onset of visual stimulus[29], visual matching task [11][41][22], cursor control [42], rapid image discrimination task [43], face detection [38][40]. Recently from 2020 to early 2021 quite a few works have been done that have versatile applications like navigation, human to human interaction, gaming and crowd source recognition [44][45][46][47]. The use of multi brain decision in defense and intelligence sector is discussed in several works [4][23], where neural correlates and reaction time of the response are used as the marker of cognitive confidence along with sigmoidal decision function.

In the above literature, though the neural correlates and other markers of human confidence is provided but any direct and analytical measure of it is missing. This paper tries to overcome such limitations by incorporating a measure of certainty a subject has during the decision making process. The certainty measure is later utilised in collaborative decision making process.

Another important aspect of the present paper is multiple decision fusion in a dynamic environment. Decision fusion uses a data reduction technique to map the multiple inputs to a lesser number of inputs. Among the existing decision fusion approaches, linear and log opinion pool generates a probability distribution as the output but drawback of the linear tool is that the distribution is multi-modal[48]. The log opinion tool though generates the unimodal output distribution but any input model assigning zero probability would restrict the final output to zero [48]. Voting technique is also extensively applied in the opinion fusion literature such as majority voting [49], rank based voting[50] but these methods are not able to handle the numerical scores (in our case it is certainty value) to generate consensus.

Decision fusion at classifier stage is also explored with an aim to combine the different classifier outputs for a single task. Classifier ensemble has an advantage of better generalization capability but this technique is suitable when the input pattern have similar response to a given class label [51]. As in our case the subjective response varies greatly with individual certainty and experience, the above technique is not the appropriate choice.

Other decision fusion methods based on supervised and unsupervised learning learning provides a trade off between detection rate and false alarm [52][53][54]. Apart from it such methods do not account any parameter for subjective accuracy or certainty that governs the final class label. Among the other opinion fusion technique, Dempster-Shafer (DS) [55] and Fuzzy decision are both able to handle the uncertainty in decision making but in case of DS the generation of mass function exponentially increases the complexity with addition of new element in the frame of discernment and it doesn't also provide any definite strategy for conflicting beliefs [56], whereas the requirement of prior experience to construct the fuzzy membership function limits the use of Fuzzy decision

fusion in this present context [57].

Group decision making for strategic planning has been in existence for quite a long time. It mainly considers four possibilities under which decision is made, named as classical dynamic consensus, time modelling consensus, dynamic environment consensus and adaptive consensus [58]. Classical consensus model relies on changing the expert preference during the negotiation process [59][60]. These models work with multistage negotiation hence not suitable for real time operation. Some fast convergence models are also suggested to shorten the negotiation time and to update the information in real time, but the models are not able to capture behavioural changes [61]. In the time modelling consensus, Hagelman *et al.* proposed an opinion dynamic model which considers the social influence(opinion of other experts) during decision making, but the opinion of other experts must be known to the decision maker. In recent times Gupta *et al.*[62], Xu *et al.* [63] proposed a multi period time consensus model but the models are not ready to be implemented in real time. In order to cope up with dynamic environment, recent consensus model considers the dynamic alternatives or dynamic criteria. Such dynamic alternatives and criteria might be useful for strategic planning but imposes restriction where the chosen alternatives can not be varied. Adaptive consensus models are also proposed that adapts the amount of group recommendations to a certain degree of consensus by varying the experts importance and weightage. The model assumes that user accepts the feedback recommendations and willing to change their original preference but the assumption may not hold true for all the cases. The model also lacks of incorporating any cognitive parameters related to persuasion process. Moreover all the current GDM process do not include any analytic measure of certainty with which the subject is making decision, hence the quality of consensus is not addressed even if the consensus is reached.

III. PROPOSED METHOD

A group of subjects is appointed to detect the object of importance from a satellite image of a vast region. The subjects take part in the experiment simultaneously inside a same room and they are restricted to have any opinion exchange between them. Before conducting the experiment The group has undergone a training of the defense symbols which frequently appears in satellite image of a country border (such as military tanks, troops etc.). Satellite image appears in a big screen in front of the appointed group. All the participants are equipped with Electrooculogram (EOG) and Electroencephalography (EEG) sensors to capture eye movement activity and brain activity respectively. The participants visually scan the entire image and look for the presence of any abnormal or suspicious object. If the person has a prior idea about objects scattered over the image or if any object matches with their previously learned defense symbols; he/she does not pay any attention to those objects but if there exist any object which is not common and rarely present in the area, he/she generates the oddball brain signal P300 in response of seeing those objects. EEG sensors attached with the subject captures the P300 response and EOG sensors placed over

canthus of the eyes detect the eyeball position which in turn generates the location of the target object in the image frame under suitable calibration. The proposed system works by the method of collaborative decision fusion by considering the confidence of the subject while formulating decision. It is observed that at first glance an object might seem to be odd but after careful observation the subject gets confused about it; hence a measure of certainty is required in the decision making period. The paper proposes a novel approach to estimate the certainty level of the subject throughout the decision making process. The estimated certainty level of each subject is used in a decision fusion algorithm to combine the decision of all the group members. The subject less certain about his/her decision has lesser importance in contributing towards final decision whereas the subject with higher certainty has higher importance in contributing towards the final decision.

In the current experiment A, B, C, D, E represent the five expert members who are involved in the surveillance task. An object P (marked by red circle) appears on the satellite image as shown in Fig.1 below. All the expert members visually



Fig. 1: A Satellite Image with circled object(Imagery©2020, Maxar Technologies, Map Data Google©2020).

scan the entire image. Expert member A, B and C have prior idea of object P, resulting no odd ball signal in their brain whereas expert members D and E do not have prior experience of object P, hence occurrence of P seems to be odd for them and generates a P300 response as a consequence of odd ball signal. The object location corresponds to P300 generation is marked depending on the collaborative decision algorithm which uses the certainty of the decision as a prime factor for its final conclusion.

IV. P300 DETECTION

Discrimination between trials containing P300 evidence and trials without P300 evidence is not possible from raw EEG samples. Hence the raw EEG signal passes through a feature extraction method which extracts the most discriminative features hidden in the raw data.

The paper uses Empirical mode Decomposition (EMD) to extract the features of the raw EEG signal. EMD is most suitable for signals with a mixed scale of frequencies, where slow oscillations are superimposed with fast oscillations [64]. The main advantage of EMD is that it is data driven where the transform basis is adaptive in nature and depends on the initial sequence. EMD functions by decomposing the initial sequence into Intrinsic Mode Functions. Feature vector is

obtained for two different classes of signal ($P300(\hat{x}_1(n))$ and $No-P300(\hat{x}_2(n))$) by applying EMD algorithm to both of them. Supplemental theory of EMD is provided on Section S1.2 of supplementary material.

The Radial Basis Function(RBF) operator is used here as the unitary transformation kernel for binary classification of presence and absence of P300 signals in the brain. A feature space sensitive RBF kernel is designed here. Most discriminating feature information over a single epoch is contained around the global maxima (within the time-span of 250ms-350ms) and the data shows redundancy under consecutive local extrema points. The distance metric is selected so that the optimal weight training occurs in such a way that it uniformly spreads the non-redundant feature characteristic during the classification process. The distance metric follows the exponential distribution (follow a measure μ) because of the property of a RBF kernel and the exponential distribution spreads out data uniformly. The Euclidean distance is weighted with a factor $c \in (0, 1]$ to incorporate relative importance in the classification process. Since the P300 peak occurs at around 300 ms; c is maximum so that the corresponding EMD feature data when spread resembles Gaussian distribution. It linearly decreases after passing either side of the (250-350) ms mark. Each set of data (P300 and No-P300) projected by the RBF is separated by a linear SVM.

Every individual classifier C_i stores its output after a single time frame which is fed as input to a derived classifier for final classification. The feature signals $\hat{x}_1(n)$ and $\hat{x}_2(n)$ are designated as \mathbf{Y} and serve as input to the classifier. During the training phase the input vector \mathbf{Y} is pre-processed and fed to the first layer of the network. This full layer serves as input to the first hidden layer of N normally distributed RBFs with center vector μ and variance vector σ . The first hidden layer ϕ is mapped to the second hidden layer ψ using synaptic weight connections. The weight operator \mathbf{W} is trained using projection operator training algorithm which is the generalization of Newton-Raphson method for single basis. The output of the second hidden layer is plotted for both sets of data(Class **1**(P300) and Class **0**(No P300) over epochs. Each set of data produces a cluster over the time frame. The clusters are separated using a linear SVM. The Class center vectors of the clusters are assigned M_0 and M_1 . The second hidden layer ψ both normalize and project the RBF functions using the weight matrix. The layers are mapped using Eq.(1) and Eq.(2) given below;

$$\phi_i = \phi_i(||\mathbf{Y} - \mu_i||) = e^{\frac{-c||\mathbf{Y} - \mu_i||^2}{2\sigma_i^2}}. \quad (1)$$

$$\psi_i = \psi_i(||\mathbf{Y} - \mu_i||) = \frac{w_i \phi_i(||\mathbf{Y} - \mu_i||)}{\sum_{i=1}^N \phi_i(||\mathbf{Y} - \mu_i||)}. \quad (2)$$

Here $1 \leq i \leq N$; where N is the number of data points in the linear SVM and w_i is the corresponding weight vector element. The weight matrix \mathbf{W} is trained using local linear projection algorithm given by (3),

$$w_i(t+1) = w_i(t) + \eta[y(t) - \psi_i(\mathbf{Y}, \mathbf{W})] \frac{u_i(||\mathbf{Y} - \mu_i||)}{\sum_{i=1}^N u_i^2(||\mathbf{Y} - \mu_i||)}. \quad (3)$$

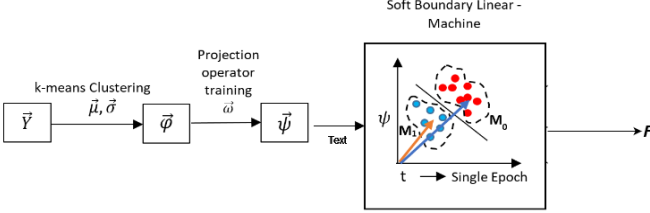


Fig. 2: Block Diagram of Individual Classification Process

Here η is the learning parameter, $y(t)$ is the reference dataset and \mathbf{u} is given by:

$$u_i(\|\mathbf{Y} - \mu_i\|) = \frac{\phi_i(\|\mathbf{Y} - \mu_i\|)}{\sum_{i=1}^N \phi_i(\|\mathbf{Y} - \mu_i\|)}. \quad (4)$$

We have considered a single classifier but the algorithm remains the same for all other classifiers. The individual classification is illustrated in Fig. 2 where F is the binary level output.

V. OBJECT LOCALIZATION USING EOG SIGNAL

Location of any object is found in terms of pixel value using Electro-occulogram (EOG) signal. EOG signal is synchronized with image frame using and artificial neural network (ANN) to decode the coordinate of the object in the satellite image. EOG uses four electrodes to capture the horizontal and vertical eye movements including the fixation and saccades [65]. Two EOG electrodes placed on outer side of the two eyes detect horizontal movement and other two electrodes were placed above and below of one eye detects vertical eye movement. EOG electrode placement is given in Fig.S4.1 in supplementary material. Eyeball position is calculated as potential difference between the horizontal and vertical pair of electrodes.

$$X_{EOG} = V_{LEFT} - V_{RIGHT}. \quad (5)$$

$$Y_{EOG} = V_{UP} - V_{DOWN}. \quad (6)$$

Equation (5) and 6 above describes the position of eyeball in terms of x and y coordinate. An artificial neural network (ANN) with back-propagation supervised learning is taken as universal approximator of the complex mapping between eyeball coordinate and pixel coordinate in the screen [66].

The entire computer screen is divided into 128x256 grids where a specific dot mark appears in each center of the grids with regular interval of 1s. Subject is asked to follow the dot marks appearing in the screen and EOG signal is captured. EOG data is recorded for 128x256 discrete points where each point corresponds to each eyeball position in terms of potential difference. An ANN architecture(shown in Fig S4.2 of supplementary material) with gradient descent based back-propagation learning, is considered in order to get the inverse horizontal and vertical eye model of human subject. Recorded EOG data along with the grid center values are used to train the network.

VI. MEASURE OF CERTAINTY

The certainty function is derived from the basic formulation of Lagrangian mechanics using the action integral. Motivated

from Landauer's principle[67], the action integral is formulated here by considering Shannon Information content as the state variable affecting the brain state transition due to external stimuli. The justification behind such a transformation is postponed till the next section. During real time operation, action measure obtained from each subject performance is compared with pre-labeled reference action measure.

A. Variational formalism of stochastic systems

As the trajectory of any EEG signal is based on the initial Information content(say I_1) generated in the brain of the subject; any extra information(I_2) entering the system(brain) will change the default trajectory which represents the subject's final decision. Generally a set of information influences the final decision of a subject. This paper establishes the idea of treating Shannon Information content $I_i = -\ln(P_i)$ (i is the subject index) as a generalised coordinate in the Lagrangian formalism.

The following assumptions are taken into account:

- 1) Abstract mass of a "particle" in Information space opposes acceleration.
- 2) The internal system force is taken constant as the free energy tends towards zero for large number of particles.

The action integral based on the Lagrangian of a system is given by:

$$S = \int_{t_1}^{t_2} \mathcal{L}(q_1, q'_1, \dots, q_n, q'_n, t) dt \quad (7)$$

$$= \int_{t_1}^{t_2} \mathcal{L}(I_1, I'_1, \dots, I_n, I'_n, t) dt \quad (8)$$

$$\mathcal{L} = T - V \quad (9)$$

where q_j denotes the generalised co-ordinate of the particles where $1 \leq j \leq n$ and q' denote the derivative. Here, T is the Kinetic Energy and V is the Potential Energy. The differential of the action integral yields:

$$\delta S = \int_{t_1}^{t_2} \sum_{j=1}^n (\partial_{I_j} - D_t \partial_{I'_j}) \mathcal{L}_j \delta I_j dt. \quad (10)$$

Here j is the particle index, $\partial_{I_j}, \partial_{I'_j}$ denotes the partial derivative w.r.t. I_j and I'_j and D_t denotes the total derivative w.r.t. time. When the necessary initial conditions are known, it is sufficient to prove that if $\delta A_j = (\partial_{I_j} - D_t \partial_{I'_j}) \mathcal{L}_j = 0 \forall 1 \leq j \leq n$, then δS becomes zero and hence S is minimum which implies the stationary condition is followed in the information space Ω . This would validate our proposition of considering Shannon Information content as a valid state variable in Lagrangian formalism. The experimental procedure supplies two ground truth curves or reference curves viz. P300 signal versus no P300 signal. The difference between the action measure of a novel EEG trial and the action measure of the reference dataset is taken as the measure of certainty. The action measure vector \mathbf{A} consists of the action measures of all the 10 participants across each stimuli in the testing session. Algorithm 1 runs for a single stimuli for each participant. As the normalised EEG signal is stochastic, the p.d.f. of

the EEG trial of a particular subject and the corresponding information content is given by (11) and (12) respectively.

$$P_i = \frac{1}{\sqrt{2\pi\sigma_i^2}} e^{-\frac{(t-\mu_i)^2}{2\sigma_i^2}}, \quad (11)$$

$$I_i = -\ln(P_i) = \frac{(t-\mu_i)^2}{2\sigma_i^2} + \frac{1}{2} \ln(2\pi\sigma_i^2). \quad (12)$$

where μ_i, σ_i is the mean and variance of the random distribution and t is the time of response of any participant across a single stimuli. From (12) we can further deduce $I'_i = \frac{(t-\mu_i)}{\sigma_i^2}$ and then $I''_i = \frac{1}{\sigma_i^2}$. Since mass is the inherent property of a particle which opposes any change in inertia caused by any external unbalanced force, mass opposes acceleration. In light of this logic, we define an abstract mass function of the information content by $m_i \propto \frac{1}{I''_i}$ where $q'' \rightarrow I''$ implies acceleration in the information space Ω . As $I''_i = \frac{1}{\sigma_i^2}$ which implies $m_i = c\sigma_i^2$ which we take as σ_i^2 . Therefore $\mathcal{L} \equiv \mathcal{L}(I, I', t); \delta A_i = (\partial_{I_i} - D_t \partial_{I'_i}) \mathcal{L}$ as the higher order terms vanish. The element Lagrangian is given by:

$$\mathcal{L}_i = \frac{1}{2} m_i (I'_i)^2 - U_i(I_i), \quad (13)$$

$$= \frac{\sigma_i^2}{2} (I'_i)^2 - U_i(I_i) \quad (14)$$

Since $F_{int} = k$;

$$-\nabla U_i = F_{int,i} = k_i. \quad (15)$$

As Information co-ordinate is only dependant on time and is one dimensional in Ω ,

$$U_i = - \int_{\Omega} F_{int,i} dI_i \quad (16)$$

$$= - \int_{\Omega} k_i dI_i \quad (17)$$

$$= -k_i I_i = -I_i. \text{(Since signal is normalised.)} \quad (18)$$

The Lagrangian is formulated as:

$$\mathcal{L}_i = \frac{\sigma_i^2}{2} (I'_i)^2 + I_i. \quad (19)$$

which implies $\delta A_i = (\partial_{I_i} - D_t \partial_{I'_i}) \mathcal{L}_i \quad (20)$

$$= \frac{\partial \mathcal{L}_i}{\partial I_i} - \frac{d}{dt} \frac{\partial \mathcal{L}_i}{\partial I'_i} \quad (21)$$

$$= \frac{\partial(\frac{\sigma_i^2}{2} (I'_i)^2 + I_i)}{\partial I_i} - \frac{d}{dt} \frac{\partial(\frac{\sigma_i^2}{2} (I'_i)^2 + I_i)}{\partial I'_i} \quad (22)$$

$$= 1 - \frac{d}{dt} (\sigma_i^2 I'_i) = 1 - \sigma_i^2 I''_i = 0. \quad (23)$$

This implies that the given random distribution satisfies the Euler-Lagrangian stationary condition in the abstract information phase space Ω . Several conclusions are in order if the random variables can be uniformly set up by normal distribution:

- The variational formalism can be used effectively on stochastic multi-body systems.
- Information can be treated as a generalised co-ordinate in the Lagrangian under the assumption of the abstract mass of the system opposing acceleration.

The second point leads to an important observation. Since there exists a framework under which we can treat Information content as a generalised co-ordinate; there must exist optimal trajectories of the same in Ω . The action integral $\int_t \mathcal{L} dt$ thus can directly lead us to a measure of certainty(confidence) of any participant.

B. Derivation of Confidence Measure

Before proceeding on to explicitly define the action measure vector, few justifications are in place. As \mathcal{L} is equal to the total energy of the system, it is alternatively the total information content of the system. The previously obtained reference dataset is used to obtain a relative certainty measure. The following mechanism ensures lower action measures correspond to higher certainty(confidence of the subject).

The action measure vector \mathbf{A} is modified to

$$A_i = \int_t \mathcal{L}_i dt \quad (24)$$

$$= \int_t \left(\frac{\sigma_i^2}{2} (I'_i)^2 + I_i \right) dt \quad (25)$$

$$= \int_t \left(\frac{\sigma_i^2}{2} \left(\frac{t-\mu_i}{\sigma_i^2} \right)^2 + \frac{(t-\mu_i)^2}{2\sigma_i^2} + \frac{1}{2} \ln(2\pi\sigma_i^2) \right) dt \quad (26)$$

$$= \int_t \left(\frac{(t-\mu_i)^2}{\sigma_i^2} + \frac{1}{2} \ln(2\pi\sigma_i^2) \right) dt \quad (27)$$

$$= \frac{(t-\mu_i)^3}{3\sigma_i^2} + \frac{1}{2} \ln(2\pi\sigma_i^2) t. \quad (28)$$

We will substitute $t \rightarrow t_i$; where t_i is the response time of any participant per stimuli. The modulus of the difference between \mathbf{A} and \mathbf{G} gives the uncertainty value of a participant for a single session, where \mathbf{G} is the action measure of reference dataset obtained similarly as \mathbf{A} . The measure of certainty of an individual participant is defined in %age as

$$Q_i = 100 \left(1 - \frac{|A_i - G|}{G} \right).$$

Here \mathbf{Q} is the Certainty Vector. The following pseudo-code provides a general procedure to calculate confidence measure vector for each stimuli across the whole session.

Algorithm 1: Certainty Measure

Map the EEG time series of each participant across a single session by the $\mathcal{N}(\mu, \sigma)$ distribution.

$\forall i; \exists t_i, \mu_i, \sigma_i$ such that $I_i = \frac{(t_i-\mu_i)^2}{2\sigma_i^2} + \frac{1}{2} \ln(2\pi\sigma_i^2)$.

$\forall i; \exists$ a unique Lagrangian $\mathcal{L}_i = \frac{\sigma_i^2}{2} (I'_i)^2 + I_i$.

Calculate the stationary action for each participant

$A_i = \frac{(t_i-\mu_i)^3}{3\sigma_i^2} + \frac{1}{2} \ln(2\pi\sigma_i^2) t_i$.

if Signal is P300 positive **then**

Calculate the Certainty Measure: $Q_i = 100 \left(1 - \frac{|A_i - G_p|}{G_p} \right)$.

else

Calculate the Certainty Measure: $Q_i = 100 \left(1 - \frac{|A_i - G_{np}|}{G_{np}} \right)$.

end if

When the local A_i measure is very high; it generally always signifies the wrong decision in a particular trial. The deviation $|A_i - G|$ is significant and for cases $\frac{|A_i - G|}{G} > 1$; we take null value for confidence.

VII. THEORETICAL JUSTIFICATION FOR LAGRANGIAN ACTION AS AN ACCURATE MEASURE

This section aims to theoretically deduce how the Lagrangian action in Shannon Information Space is a reliable measure of confidence for stochastic multi-decision fusion algorithms.

A. Derivation of the Lagrangian Measure

The expected Kinetic $\langle T \rangle$ and Potential $\langle V \rangle$ Energy of a particle in generalised co-ordinate space(q) over time τ are given by,

$$\langle T \rangle = \frac{\int_0^\tau T dt}{\int_0^\tau dt} = \frac{\int_0^\tau \frac{1}{2}m(\dot{q}(t))^2 dt}{\tau}. \quad (29)$$

$$\langle V \rangle = \frac{\int_0^\tau V dt}{\int_0^\tau dt} = \frac{\int_0^\tau V dt}{\tau}. \quad (30)$$

The variational derivative of a functional $F(q(t))$ at any $t = t_0$ is given by

$$\lim_{\epsilon \rightarrow 0} \frac{F(q(t) + \epsilon \delta(t - t_0)) - F(q(t))}{\epsilon}.$$

Here $\delta(t)$ is the Dirac delta function. The variational derivatives $\frac{\delta \langle T \rangle}{\delta q}$ and $\frac{\delta \langle V \rangle}{\delta q}$ give;

$$\begin{aligned} \frac{\delta \langle T \rangle}{\delta q} &= \frac{1}{\tau} \lim_{\epsilon \rightarrow 0} \frac{1}{\epsilon} \int_0^\tau \frac{1}{2}m(q'(t) + \epsilon \delta'(t - t_0))^2 - \frac{1}{2}m(q'(t))^2 dt \\ &= \frac{1}{\tau} \lim_{\epsilon \rightarrow 0} \frac{1}{\epsilon} \int_0^\tau \frac{m}{2}((q' + \epsilon \delta'(t - t_0))^2 - q'^2) dt \\ &= \frac{m}{2\tau} \lim_{\epsilon \rightarrow 0} \frac{1}{\epsilon} \int_0^\tau (\epsilon^2 \delta'^2 + 2\epsilon \delta' q') dt = \frac{m}{2\tau} \int_0^\tau (2\delta' q') dt \\ &= \frac{m}{\tau} \left(q' \delta(t - t_0) - \int_0^\tau q'' \int_0^\tau \delta' dt \right) = 0 - \frac{m}{\tau} \int_0^\tau q'' \delta dt \\ &= -\frac{mq''(t_0)}{\tau}. \end{aligned}$$

$$\begin{aligned} \frac{\delta \langle V \rangle}{\delta q} &= \frac{1}{\tau} \lim_{\epsilon \rightarrow 0} \frac{1}{\epsilon} \int_0^\tau \left(V[q(t) + \epsilon \delta(t - t_0)] - V[q(t)] \right) dt \\ &= \frac{1}{\tau} \lim_{\epsilon \rightarrow 0} \frac{1}{\epsilon} \int_0^\tau V[q(t)] + \epsilon \delta(t - t_0) \partial_q V[q(t)] + O(\epsilon^2) \\ &\quad - V[q(t)] dt \\ &= \frac{1}{\tau} \int_0^\tau \delta(t - t_0) \partial_q V[q(t)] dt = \frac{\partial_q V[q(t_0)]}{\tau}. \end{aligned}$$

Since a classical particle always follow $mq'' = -\partial_q V[q(t)]$; it implies that $\frac{\delta \langle V \rangle}{\delta q} = \frac{\delta \langle T \rangle}{\delta q}; \forall t_0 \in [0, \tau]$. This equation can be re-written as $\frac{\delta \langle T \rangle - \delta \langle V \rangle}{\delta q} = \frac{\delta}{\delta q} \left(\int_0^\tau (T - V) dt \right) = 0$. This expression furnishes the stationary Lagrangian measure $S = \int_0^\tau \mathcal{L} dt$. The condition $\frac{\delta S}{\delta q} = 0$ is sufficient for the optimal trajectory of a particle and it leads to $(\partial_q - \frac{d}{dt} \partial_{q'}) \mathcal{L} = 0$. This aims to show how the idea behind choosing \mathcal{L} as an initial choice for certainty measure was conceived.

B. Analysis

The classical principle of least action fails for random statistical systems like weather dynamics, neural processing etc because of incomplete information on the system. Assuming each path having distinct action measures with corresponding path probabilities; the expected action measure $\langle S \rangle = \sum_{x=1}^N p_{if}(x)S_{if}(x)$ is taken over all paths; where i, f are the initial and final points in the trajectory and $x \in [1, N]$ is the path index. The mean of variations for all the paths $\langle \delta S \rangle$ becomes;

$$\begin{aligned} \langle \delta S \rangle &= \sum_x p_{if}(x)\delta S_{if}(x) \\ &= \delta \sum_x p_{if}(x)S_{if}(x) - \sum_x \delta p_{if}(x)S_{if}(x) \\ &= \delta \langle S \rangle - \sum_x \delta p_{if}(x)S_{if}(x) \\ \implies \delta E &= \sum_x \delta p_{if}(x)S_{if}(x) = \delta \langle S \rangle - \langle \delta S \rangle. \end{aligned} \quad (31)$$

The physical quantity defined as δE has a balanced trade-off with the mean variation $\langle \delta S \rangle$ as $\delta \langle S \rangle$ is the variation of total measure of energy in the system. Eq.(31) also closely resembles the first law of thermodynamics as $\langle \delta S \rangle = \sum_x p_{ij}(x)\delta S_{if}(x) = \sum_x p_{ij}(x)\frac{\partial S}{\partial q} := -\delta W$ can be viewed as external work done by the system. A simple conclusion follows that the term δE must correspond to the total internal energy or entropy of the system needs to be maximum for the most stable evolution of the stochastic process; i.e. $\langle \delta S \rangle = 0$. A parallel viewpoint is provided by Jayne's principle of maximum entropy[68] which gives $p_{if}(x) \propto e^{kS_{if}(x)}$ as the optimal probability distribution. The normalisation of the probability distribution leads to $p_{if}(x) = \frac{e^{kS_{if}(x)}}{Z}$ where $Z = \sum_x p_{if}(x)$ is widely known as the partition function. A detailed exposition on how the principle of maximum entropy is equivalent to the stochastic least action principle can be found in [16][17]. The equivalence of the two physical principles and the subsequent maximisation of path entropy leads to an exponential distribution. The most stable path of evolution in any stochastic system in generalised co-ordinate space is then given by the stochastic path of least action characterised by the maximum entropy principle. But one observes that path entropy $H_{if} = \sum_x p_{if}(x)S_{if}(x)$ under the optimal distribution changes to Shannon Information Entropy;

$$\begin{aligned} H_{if} &= \sum_x p_{if}(x)S_{if}(x) \\ &= \sum_x \exp(kS_{if}(x))S_{if}(x) = k \sum_x p_{if}(x) \ln p_{if}(x). \end{aligned} \quad (32)$$

As action is minimum for $\forall k < 0$; Eq.(32) turns into Information Entropy as shown in [16]. This framework of conversion from physical path entropy to Information entropy is very useful for further deduction since this leads to a direct duality between the most stable path evolution given by stochastic least action path in q - space and the most discriminate Information content features in Information space Ω . Since $\max_{q-space} H_{if}$ is equivalent to $\max_{\Omega} H_{if}$; minimising action automatically implies Lagrangian action in Ω . The

most stable set of paths is the maximum informative set of signals(paths) in Ω leading to original evolution of the physical system because of the duality between generalised co-ordinate space and Ω . This justifies the reasoning behind assuming the Lagrangian action measure in Ω as similar to physical co-ordinate space. As the most stable set of trajectories in Ω is most informative; the measure of confidence in the preceding section is an accurate measure of certainty.

VIII. COLLABORATIVE FRAMEWORK FOR MULTI-SUBJECT DECISION FUSION

Collaborative decision fusion framework is depicted in Fig.3. The first layer \mathbf{F} is the final output of each individual classifier after one-time window, the second layer (\mathbf{P}) is the Class Center of ψ_l as computed by the SVM and the third layer \mathbf{Q} contains the confidence/certainty measure for each participant in the group. The layer \mathbf{D} stores the separation

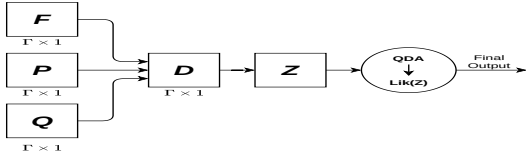


Fig. 3: Collaborative Decision Fusion Scheme

distance of \mathbf{P} from the Class Center of \mathbf{F} . The Q-measure is incorporated in such a way that it influences the collaborative decision by acting as a measure of variance in layer \mathbf{Z} . The relationship is given below,

$$\begin{aligned} D_l &= \|Q_l^{-1}(\mu(\psi_l) - F_l)\|. \\ &= \|Q_l^{-1}(P_l - F_l)\|. \end{aligned} \quad (33)$$

$$\because Q_l \in \mathcal{R}; D_l = Q_l^{-1}\|(P_l - F_l)\|.$$

Here μ is the class center of ψ_l and $\|\cdot\|$ is defined by a modified L^p norm given by;

$$\|a, b\| = d(a, b) = \left(\sum_i (a_i - b_i)^{2p} \right)^{\frac{1}{2p}}$$

$\forall p, k \in \mathcal{N}$ and $1 \leq i \leq k; \exists a_i, b_i \in [0, 1] \implies a, b \in \mathcal{R}^k[0, 1]$. Here we prove that it is a valid distance metric. Proof is given in the section S2.1 of Supplementary Material.

The elements of layer \mathbf{D} can be represented as:

$$\begin{aligned} D_l &= Q_l^{-1}\|P_l - F_l\|. \\ &= Q_l^{-1} \left(\sum_i^N \{(P_l)_i - (F_l)_i\}^{2p} \right)^{1/2p}. \end{aligned} \quad (34)$$

Here, $(F_l)_i$ is either 1 or 0 and $\psi_l \in \mathcal{R}^N$. This process helps in incorporating confidence measures of everyone in the group to affect the collaborative decision fusion effectively.

The layer \mathbf{D} is fed as input to the layer \mathbf{Z} as:

$$\begin{aligned} Z_l &= \frac{1}{\sqrt{2\pi}} e^{\frac{-D_l^2}{2}}. \\ &= \frac{1}{\sqrt{2\pi}} e^{\frac{-\left(\sum_i^N \{(P_l)_i - (F_l)_i\}^{2p} \right)^{1/2p}}{2Q_l^2}}. \end{aligned} \quad (35)$$

It must be noted that QDA allows a weighted voting mechanism, which means that it is a performance driven classifier because as D_l increases, Z_l decreases and thus has significantly less effect on the QDA. Hence the best performing classifier has the most significant influence on the QDA Objective function which is given below,

$$Lik(\mathbf{Z}) = \frac{\sqrt{[2\pi \sum_{x=1}^{-1}] e^{-\frac{(\mathbf{Z}-\mu_{x=1})^T \Sigma_{x=1}^{-1} (\mathbf{Z}-\mu_{x=1})^T}{2}}}}{\sqrt{[2\pi \sum_{x=0}^{-1}] e^{-\frac{(\mathbf{Z}-\mu_{x=0})^T \Sigma_{x=0}^{-1} (\mathbf{Z}-\mu_{x=0})^T}{2}}}}. \quad (36)$$

Here Σ is the Covariance Matrix and μ is the mean which are obtained from individual classifier data averaged across the subjects in each group. The collaborative classifier is trained using datasets having final output Classes 1 and 0. The Objective function used is a local likelihood function tested against a threshold parameter θ_0 . Algorithm 2 selects the final output(X) from the QDA classifier which works at decision fusion level and the threshold parameter θ_0 is chosen without bias towards any of the binary classes.

Algorithm 2: Collaborative Classification

```

if Lik(Z) > θ₀ then
  X ← Class 1.
else if Lik(Z) < θ₀ then
  X ← Class 0.
else
  for l=1 to T in steps of 1 do
    if F_l == Class 1 then
      c₁ ← c₁ + 1.
    else
      c₂ ← c₂ + 1.
    end if
  end for
  if c₁ > c₂ then
    X ← Class 1.
  else
    X ← Class 0.
  end if
end if
  
```

IX. EXPERIMENT AND RESULTS

This section describes the detailed protocol undertaken for the experiment and the results obtained during the experiment. Experiment is conducted in two sessions; firstly the training session is conducted with individual subjects whereas the collaborative decision fusion is done in the testing session. Performance analysis of the individual and collaborative classifiers is shown with various metrics obtained from Confusion matrix. A total of 10 subjects participated in the training session and 6 among them are male and rest are female. Testing session is validated with simultaneous participation of 5 subjects. All of the subjects are in the age group of 18-30. Medical history of the volunteers shows no major disease or any major surgery in recent past. Details of aim and objective of the experiment was made clear to them before they participate in the study. A consent form, stating their willingness to take part in the study, were duly signed by the subjects. All other safety and ethical issues are maintained according to the Helsinki Declaration of 1970 revised later in 2000 [69]. Ethical Clearance is also obtained from Hurip Independent Bioethics Committee having registration no ECR/103/Indt/WB/2013/RR-19.

A. Signal Acquisition

EEG and EOG signals are acquired using 32 channel EEG acquisition system made by Nihon Kohden. Sampling frequency of the amplifier is 200 Hz. EEG electrodes are placed using international 10-20 convention. The amplifier uses A1 and A2 electrode position as reference and Fp1 position as ground. Here three electrodes Fz, Cz, and Pz are considered. Amplifier uses a 50 Hz notch filter to eliminate the disturbance arising from power line frequency.

B. Training Session

Training data are obtained for 10 subjects with repetition of four sessions each day for each subject throughout the 15 days. Before conducting the experiment, ten defense symbols are presented before the subjects and asked to observe the symbols carefully. Now the subjects are asked to seat comfortably in front of a screen where the visual stimuli appear. Timing diagram of visual stimuli presentation is illustrated in Fig.4. The visual stimuli contain defense symbols embedded in a satellite image, where some symbols appear exactly in the form it appeared in the previous list shown to the subject and some of the symbols appear in distorted form. Symbols are distorted to invoke possible confusion. Some of the satellite image also contain symbols which are not present in the list. P300 response can be developed in either of the two cases, first if the subject sees any foreign object that was not contained in the symbol list and second if the subject fails to identify any known symbol due to distortion. The later case contributes towards false positive rate. The present training scheme generates the training dataset of P300 classifier and records the individual cognitive confidence.

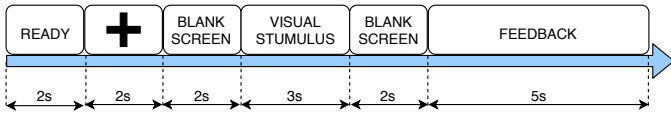


Fig. 4: Visual Stimuli timing diagram

Training session also includes subjective EOG calibration where a positional offset between actual object location and measured location is corrected for individual subjects. The detailed EOG calibration procedure is explained in Section S1.2 of Supplementary material and EOG calibration result is presented in Table S3.1 and in Fig S4.3 of supplementary material , where performing *t* test on each pair of actual and calibrated signal shows no statistically significant difference ($p > 0.05$). Positional offset is corrected each time the subject takes part in the experiment.

C. Training Data set preparation for certainty measure

At the beginning of the experiment a fixation cross of 2s duration appears in the screen, which is followed by a blank screen of 2s duration. The visual cue(defense symbol embedded in satellite image) is presented thereafter with 3s duration which is again followed by a blank screen of 2s duration. Now a feedback screen appears with 5s duration. The experts are asked to carefully observe if there is any

object seems suspicious to them. They are also asked to provide a feedback in 5 point scale on how confident they are about the decision during the feedback period. They are also asked to manually register their feedback by pressing the designated key in a computer keyboard as soon as they reach a conclusion. We include the entire scope of confidence scale into the reference data action measure to reduce bias. A more descriptive reasoning would involve the idea of capturing the total Information pool in the system as there is a chance of the high confidence labels not being able to capture the total pool because of the subjective overconfidence. The inclusion of low confidence labels thus serves as a measure to decrease bias. We take the effective weightage of the confidence scale from the Normalised Gaussian curve such that they are separated by common difference of $\frac{\sigma}{2}$ such that the high confidence labels (3, 4, 5) are in the $[0, \sigma]$ domain for high contribution. We assume the distribution as $f(x) = e^{-\frac{x^2}{2}}$ centred at the mean. The relative contributions become $f(0) = 1, f(\frac{3\sigma}{2}) = 0.882, f(\sigma) = 0.606, f(\frac{3\sigma}{2}) = 0.324, f(2\sigma) = 0.135$ and we take the P300 positive reference action measure as $G_p = \frac{\sum_{i=1}^5 w_i G_{p,i}}{\sum_{i=1}^5 w_i}$ and the P300 negative measure as $G_{np} = \frac{\sum_{i=1}^5 w_i G_{np,i}}{\sum_{i=1}^5 w_i}$ where G_i is the corresponding Action for the given confidence scale.

According to the situation two classes (P300 and Non-P300) of brain patterns are generated during the experiment. Normalised Confidence measure is estimated separately for two classes of signal and two separate reference datasets (G_P and G_{NP}) are prepared for each class of signal. G_P represents the reference action measure of the EEG trials containing the traces of P300 and G_{NP} represents the reference action measure of Non-P300 EEG trials. The details scheme of selecting the trials are illustrated in Fig.5. Estimated certainty value determines the weightage of his/her decision to be given in collaborative final decision.

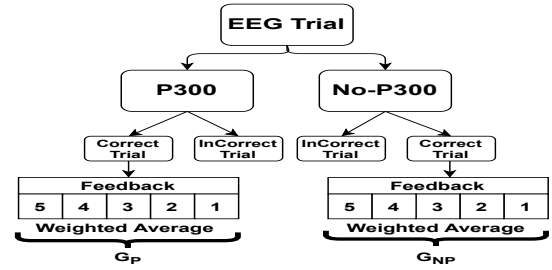


Fig. 5: Illustration of reference data set preparation

D. Testing Session

During the training session each subject participated in the experiment individually whereas in the testing session subject participates in the experiment in groups. Testing session is conducted in real time unlike the training session. Out of ten volunteers that took part in the testing session, five volunteers are selected randomly to form a group. In order to remove any selection bias, five such groups are formed with replacement. Each of the groups participated in the experiment one at a time . The objective of finding the suspicious object remains unaltered from training session. It is worthwhile to mention

that any further EOG calibration is avoided in the testing session to make the system work in real time. Ultimate decision of marking the object as an target object is governed by the collaborative multi-subject decision fusion algorithm discussed above.

E. Experimental Results

The present experiment consists of two stages. In the first stage EEG data obtained from individual participants are classified to check the presence of P300 brain pattern and the output of the trials are labeled with 1 and 0 according to the presence and absence of P300 respectively. In the second stage all the trials having class label 0 and 1, passes through a collaborative classifier. The collaborative classifier generates a final decision whether the concerned object should be marked. Single sample t - test reveals no such difference of P300 peak latency between extracted P300 samples and population mean. A signal level analysis is presented in Fig.6. Fig.6(a) represents P300 brain pattern of 5 randomly selected trials from the training session along with the population mean. Fig.6(b) and Fig.6(c) shows the comparison between correct trial (confident) and in-correct (in-confident) trial for P300 and No-P300 category respectively.

During the training session certainty measure Q is determined

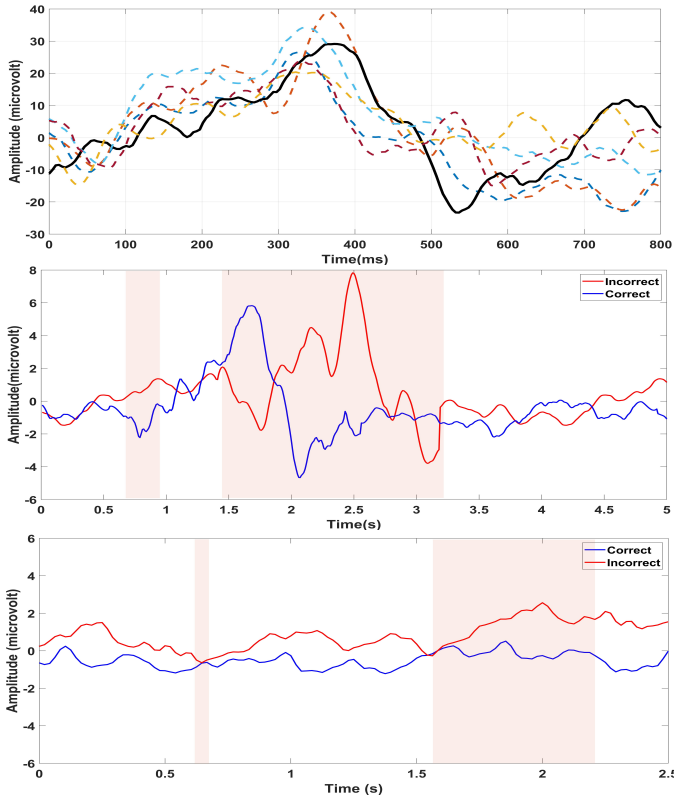


Fig. 6: (a)P300 brain pattern taken from 5 random trials and the grand average is shown in black. (b) Example of Correct and Incorrect P300 trials (c) Example of Correct and Incorrect No-P300 trial. Shaded region shows statistically significant difference ($p < 0.05$, Wilcoxon two tailed signed rank test). for every subject and every trial. The subjective Q value for each feedback rating (range:5-1) is determined by taking the

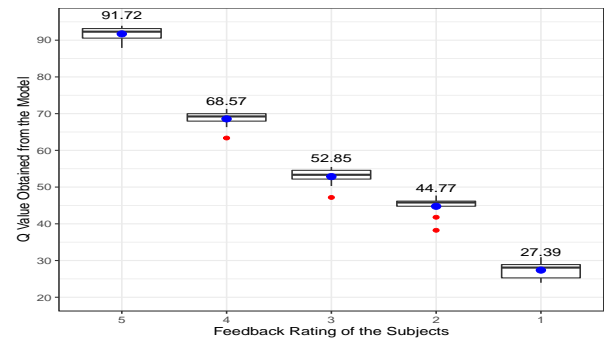


Fig. 7: Box plot of the Q values obtained for various feedback rating. Red dots represents the outliers and blue dot represents the mean value. Mean values are shown adjacently.

average of the Q values obtained from the trials in which the subject provided that rating. The result is given in Table I, where Q value for the different feedback rating is shown for each individual subject. Grand average of the Q value along with the standard deviation for each feedback rating is shown in Fig.7. In order to assess the efficacy of our confidence model to represent subjective confidence, we check the association between Q values and subjective feedback rating as listed in Table S4.6. A non-parametric measure of Spearman's-Rank correlation is employed to check the association between these two variables. Spearman's-Rank Correlation coefficient is found to be (ρ_{SR}) = 1 ($p < 0.02$), which shows a strong monotonic association between Q values and subjective confidence. The result is substantiated by evaluating Kendall tau rank correlation coefficient. The Kendall's coefficient is found to be $\tau=1$ ($p < 0.05$) which shows strong statistical dependency between Q values and subjective confidence. Classification results are expressed in terms of five common metrics obtained from Confusion matrix[70]. Metrics are Classification Accuracy (CA), True Positive Rate (TPR), True Negative Rate (TNR), Cohen's kappa.

TABLE I: Subject wise average of certainty measure (Q value) for different level of user feedback ranging from 1-5

Sub Id	Avg Q value for feedback Scale 1-5				
	Avg Q Value for feedback rating 5	Avg Q Value for feedback rating 4	Avg Q Value for feedback rating 3	Avg Q Value for feedback rating 2	Avg Q Value for feedback rating 1
Sub1	93.17	69.23	52.80	46.25	28.08
Sub2	92.0	69.76	53.90	45.89	29.51
Sub3	89.32	66.33	47.18	38.24	19.89
Sub4	93.31	70.06	54.21	44.65	24.95
Sub5	90.56	68.29	52.36	45.72	25.53
Sub6	87.20	63.36	50.30	41.79	26.27
Sub7	91.38	70.28	55.48	46.29	29.9
Sub8	92.1	69.24	54.68	45.19	28.76
Sub9	93.22	67.85	52.12	45.96	29.82
Sub10	95.02	71.28	55.48	47.70	30.91
Mean	91.72	68.56	52.85	44.76	27.39
Sd	2.25	2.29	2.57	2.75	3.49

Apart from the metrics mentioned above, another two metrics viz. geometric mean (GM) and Adjusted F-measure(ADF) [71] are included here for practical reasons. As P300 is

TABLE II: Group wise Collaborative Classification Result

Subject Id	GM%	ADF	kappa	Group Decision Algorithms									
				Q c-BCI Classifier			c-BCI Classifier			Majority Voting			
Group 1													
Sub1	89.03	0.88	0.68					91.17	0.92	0.87	89.12	0.86	0.80
Sub2	85.14	0.85	0.69										
Sub8	86.22	0.88	0.64	96.88	0.98	0.94							
Sub6	88.09	0.91	0.84										
Sub10	88.26	0.84	0.69										
Group 2													
Sub2	88.16	0.89	0.69					89.49	0.91	0.87	86.29	0.88	0.74
Sub5	85.42	0.81	0.70										
Sub6	87.28	0.82	0.66	94.84	0.96	0.95							
Sub7	81.98	0.84	0.67										
Sub9	85.34	0.85	0.66										
Group 3													
Sub1	86.26	0.86	0.68					91.24	0.90	0.81	88.19	0.89	0.72
Sub3	89.11	0.86	0.70										
Sub4	89.18	0.89	0.70	97.15	0.96	0.96							
Sub5	87.29	0.88	0.61										
Sub8	91.08	0.89	0.71										
Group 4													
Sub4	90.05	0.87	0.66					92.44	0.93	0.88	90.24	0.90	0.72
Sub6	88.21	0.86	0.64										
Sub8	89.17	0.88	0.70	97.81	0.97	0.95							
Sub9	89.22	0.89	0.70										
Sub10	88.68	0.90	0.69										
Group 5													
Sub1	89.36	0.89	0.72					92.19	0.93	0.88	90.43	0.89	0.75
Sub2	89.98	0.88	0.71										
Sub4	88.24	0.88	0.71	96.78	0.98	0.95							
Sub7	89.34	0.88	0.74										
Sub5	89.19	0.85	0.74										

generated by a rare occurring phenomenon, usually non P300 classes are higher in number than the P300 classes. Hence, Geometric Mean (GM) provide better results being insensitive to such class imbalances. It is also observed that in real life defence scenarios where the aim is to detect suspicious objects present in the battle field, the cost of false negative(FN) instances are much more higher than any other error. In order to take this into account, adjusted F-measure metric is included in the result. The metric boosts the FN values when deciding the error rate. The formal definitions of all the metrics used here is given in Section S1.3 of Supplementary material.

Table III provides a comparative analysis (averaged over all subjects across all sessions) between proposed RBF SVM classifier and other standard classifiers frequently used in the BCI literature. Subject wise detailed analysis is given in Section S1.4 and in Table S3.2 of Supplementary material. Here the Linear Support Vector Machine(LSVM) [70], RBF kernel based SVM[72], k-Nearest Neighbor(k-NN)[73] and Back Propagation Neural Network(BPNN)[74] are considered for comparison.

TABLE III: Comparison of Classifiers

Algorithm	CA(%)	TPR	TNR	GM(%)	ADF	kappa	Time(s)
SVM	86.21	0.84	0.89	87.19	0.86	0.70	0.319
RBF-SVM	92.42	0.88	0.93	92.64	0.90	0.79	0.391
Proposed RBF	95.68	0.95	0.97	96.06	0.94	0.88	0.519
k-NN	86.18	0.81	0.89	85.22	0.83	0.67	0.289
BPNN	85.13	0.81	0.82	84.49	0.82	0.63	0.311

It is evident here that the proposed RBF kernel based classifier has outperformed the other classifiers in terms of all the metrics listed in the table except the computation time which is bit higher than the rest. Average classification accuracy is increased by 3.26% with respect to the nearest competitor, whereas GM has a significant rise of 3.42%.

Individual and group performance are measured in terms of three metrics viz. GM, ADF and kappa. Performance of three

group classifier algorithms, i.e, proposed group classifier with confidence metric (Q-cBCI), proposed group classifier without confidence measure (cBCI) and Majority voting based classifier[12], along with the individual performance of participating subjects are summarised in Table II. The majority voting based classifier assigns the final class label based on majority of classes obtained from the individual classification process. In group 1, highest group GM value is obtained as 96.88%, highest group ADF is 0.98 and highest kappa value is obtained as 0.94 for the proposed group classifier that includes the confidence metric. Clearly the values are higher than the other group classification algorithms and also higher than the values obtained from individual performance. A similar trend is seen to be followed by the rest of the groups. In group 2, proposed group classifier achieves the best GM value of 94.84%, ADF value of 0.96 and kappa value of 0.95. Group 3 provides best GM, ADF and kappa as 97.15%, 0.96 and 0.96 respectively with the proposed Q-cBCI classifier, whereas group 4 provides the value of above metrics as 97.81%, 0.97 and 0.95 respectively. In group 5, Q-cBCI classifier fetches the group GM value of 96.78%, ADF as 0.98 and kappa value of 0.95. On average GM, ADF and kappa score are increased by 5.39%, 5.20% and 8% respectively. It is evident from the result that in each case the Q-cBCI classifier outperforms the ordinary cBCI classifier which does not take the confidence metric into account and also outperforms the majority voting technique.

F. Reliability Analysis under faulty condition

A separate experiment is conducted to assess the reliability of the collaborative classifier under faulty conditions. The experiment assesses the robustness of the algorithm when the performance of one or more than one participants are not up to the level. Here the total participants are divided into two groups consisting of five members in each group. The first

group is shown another set of symbols which are not disclosed to the other group. We designate the first group as expert team (ET) as they receive the prior idea of the symbols, and the second group is designated as novice team (NT) as they do not have any idea of those specific symbols. Three different categories of pools are formed by varying the number of representations from expert and novice team. The first category of pool (Pool1) includes 4 members from ET and one member from NT. The second category of pool (Pool2) includes 3 members from ET and 2 members from NT, where as the third pool (Pool3) includes 2 members from ET and 3 members from NT. Members are chosen randomly for every testing session. Five such testing sessions(10 trials x 20 stimulus) are conducted for each category and hence five different group performance is obtained under each pool category. A total of 15 group performances are obtained cumulatively.

Reliability of the system is analysed under two collaborative decision fusion algorithms i.e traditional cBCI and proposed Q-cBCI algorithm. We use cohen's kappa statistic and One way random model Intra Class Correlation coefficient (ICC1) to assess the reliability of the system, where the kappa score measure the inter rater reliability of the system and ICC measures the consistency of the accuracy obtained over the multiple sessions for a same group. The result is presented in Table IV.

TABLE IV: Reliability Analysis of group performance subjected to different decision fusion algorithm under fault condition

Group Id	Group Decision Algorithms					
	Q c-BCI Classifier		c-BCI Classifier			
	Group Acc	Group kappa	Group ICC	Group Acc	Group kappa	ICC
Pool 1 (E=4, N=1)						
Group1	94.21	0.92	0.89	85.25	0.91	0.81
Group2	93.18	0.94	0.92	86.23	0.88	0.84
Group3	91.22	0.91	0.89	85.21	0.88	0.80
Group4	92.95	0.92	0.90	85.03	0.86	0.76
Group5	92.56	0.91	0.85	83.19	0.90	0.82
Pool 2 (E=3, N=2)						
Group1	89.87	0.88	0.78	82.21	0.78	0.54
Group2	90.37	0.87	0.82	79.36	0.82	0.68
Group3	90.10	0.90	0.84	82.82	0.80	0.72
Group4	91.69	0.91	0.82	83.91	0.74	0.59
Group5	89.36	0.90	0.85	83.29	0.74	0.48
Pool 3 (E=2, N=3)						
Group1	87.83	0.87	0.69	69.39	0.75	0.62
Group2	84.21	0.86	0.65	76.27	0.81	0.50
Group3	85.22	0.84	0.70	66.94	0.68	0.42
Group4	84.63	0.84	0.71	72.92	0.66	0.36
Group5	84.00	0.83	0.73	78.14	0.68	0.38

Group accuracy is found to be decreasing with increase in non expert members in both the collaborative techniques. For the pool 1 and 2 average accuracy is found to be 92.82% and 90.28% for Q-cBCI and for the cBCI it is found to be 84.98% and 82.31% respectively which are significantly lower. Significant difference is seen in case of pool3 where average pool accuracy for Q-cBCI is 85.17% but remarkably goes down to 72.73% for the cBCI. Inter rater reliability value also decreases with pool effects. Mean kappa score falls from 0.92 to 0.84 for Pool1 to Pool3 respectively with Q-cBCI method, whereas in general cBCI method kappa score falls from 0.88 to 0.70. Inter-rater reliability value of the system also shows a larger dispersion effect (Coeff. of variation(CV)=10.12%) over

the pool in cBCI compared to Q-cBCI where the deviation (CV=3.68%) is quite small, hence shows the inconsistency of the reliability parameter for general cBCI method. Mean Intra group reliability is also found to be rapidly decreasing in general cBCI (pool1= 0.80, pool2= 0.60, pool3= 0.45) than it is seen in Q-cBCI (pool1=0.89, pool2=0.82, pool3=0.69). A worst-case comparison shows that ICC1 eventually falls to a minimum of 0.36 whereas Q-cBCI is able to retain its minimum at 0.65.

X. STATISTICAL VALIDATION

Statistical validation is carried out in two phases, first, we perform the statistical validation of the certainty model followed by the validation of the collaborative classifiers.

A. Statistical Validation of Certainty Model

Q values obtained from the proposed certainty model (as per Table I) for each feedback rating are statistically analyzed to check whether they bear a significant difference from each other.

As every population of Q values does not follow the normality assumption, we use a non-parametric test (Kruskal-Walis) to analyze any statistical difference. The test assumes a null hypothesis that all the population medians are equal and the following statistic is calculated,

$$H = \left[\frac{12}{n(n+1)} \sum_{j=1}^l \frac{T_j^2}{n_j} - 3(n+1) \right] \quad (37)$$

where n = sum of sample sizes, l = number of samples, n_j =size of the j^{th} sample and T_j = sum of ranks in j^{th} sample. If the corresponding critical Chi-Square value is less than the H statistic, the null hypothesis is rejected.

For L number of population, the test is carried out for;

$$H_0 : \mu_1 = \mu_2 = \dots = \mu_L \quad \text{vs} \quad H_1 : \mu_l \neq \mu_m$$

for at least one pair l,m.

Statistic value $H = 46.97(p < 0.01)$, $df = 4$ shows population of Q values bears a statistically significant difference. A large eta squared value $\eta^2 = 0.95$ reveals that 95% of the subjective variance is explained by the proposed model. Further a Wilcoxon pair wise test with Bonferroni's p value correction is conducted to find the significant difference between each population levels. The result shows that every pair of Q population bears statistically significant difference from each other, which ensures that the proposed certainty model performs well to represent the distinct subjective feedback rating. The Wilcoxon test result is presented pictorially in Fig.8 and the details test result is given in Table S3.3 of supplementary material.

B. Statistical Validation of Collaborative Classifiers

Multivariate Analysis of variance [75] is carried out to find the statistically significant difference between the performance of group classifiers while considering the three metrics(i.e. GM, ADF and Kappa) simultaneously.

Let any general observation x_{ij} , where $i = 1, \dots, L$ and $j = 1, \dots, m$, represent a p -dimensional performance vector where p

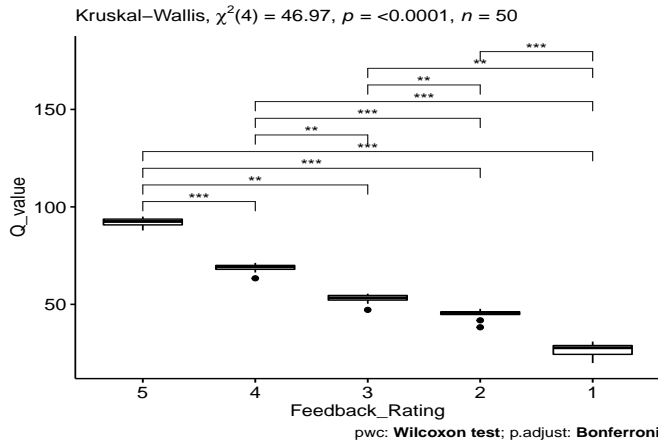


Fig. 8: Results of Wilcoxon test performed on Q values after Kruskal-Wallis test

is the number of parameters for each population. Here $L = 3$ denotes the number of population under comparison and it denotes the number of group classifiers. Multivariate analysis of variance computes the two matrices of intra-population and inter-population as described below;

$$S_B = m \sum_{i=1}^L (\bar{x}_i - \bar{x})(\bar{x}_i - \bar{x})^T \quad (38)$$

$$S_W = \sum_{i=1}^L \sum_{j=1}^m (\bar{x}_{ij} - \bar{x}_i)(\bar{x}_{ij} - \bar{x}_i)^T \quad (39)$$

for $p = 3$, $L = 3$ and $m = 5$, Λ' calculated below is Wilks' Λ distributed with $p, L - 1, L(m - 1)$.

$$\Lambda' = \frac{|S_B|}{|S_B + S_W|} \quad (40)$$

The null hypothesis H_0 is rejected if $\Lambda' \leq \Lambda_{\alpha, p, L-1, L(m-1)}$. The Wilks' Λ closely follows χ^2 distribution if approximated as below;

$$\left(\frac{p - n + 1}{2} - m \right) \log \Lambda_{p, k, n} \sim \chi_{np}^2 \quad (41)$$

The assumption of univariate normality is assessed using the Shapiro-Wilk test. It is found that each variable in each population follows normal distribution ($p > 0.05$). Homogeneity of variance and co-variance matrices are assessed using Box's M test. The test does not produce any statistically significant result ($\chi^2 = 16.4, df = 12, p = 0.18$), hence the assumption of homogeneity of variance-co-variance matrices holds in this case.

The multivariate analysis of variance with $test statistics = 0.023, F = 18.43, p < 0.01$ clearly shows the significant difference of mean values between the populations. Hence the classifier performance statistically differ from each other. MANOVA test is followed by multiple pairwise comparison between the populations to determine which populations bears any significant difference. The paper uses Tukey post-hoc test to find the difference. Tukey test result is summarized in Table V.

TABLE V: Tukey Test Result

Parameter	Comparing Group1	Comparing Group2	p value	Decision
AGF	pr1	pr2	0.00036	S
AGF	pr1	pr3	0.00031	S
AGF	pr2	pr3	0.00116	S
GM	pr1	pr2	0.00007	S
GM	pr1	pr3	0.00005	S
GM	pr2	pr3	0.04800	S
kappa	pr1	pr2	0.00540	S
kappa	pr1	pr3	0.00009	S
kappa	pr2	pr3	0.00013	S

Univariate one way ANOVA examination with Bonferroni's multiple testing correction on each three dependent variables are carried out separately to identify the parameters contributing towards global significant effect [76]. Results are listed in Table VI. It is evident from the results that each clas-

TABLE VI: Univariate One way ANOVA Results

Parameters	Dfn	Dfd	F	p
GM	2	12	56.3	$p < 0.01$
ADF	2	12	47.9	$p < 0.01$
kappa	2	12	84	$p < 0.01$

sifier performance bears a statistically significant difference from each other and all three parameters have significant contribution towards this performance. Hence the classifier performance can be ranked as per the cumulative rank obtained from each individual parameter performance. Here classifiers performance is ranked as per the following rule, higher the value of parameter lower the rank the classifier gets and the classifier having got the lowest cumulative rank is considered as the best. The rank table is summarised in Table S3.4 of supplementary material. It is evident from the above table that Q-cBCI classifier has got the lowest cumulative rank, hence it can be considered as best performing classifier in this present context.

XI. CONCLUSION

The present study provides a general framework of multi expert opinion fusion using collaborative BCI approach. The particular scheme proves to be suitable for suspicious object detection from real time satellite image by a group of defense experts. Although the scheme can be extended for any group activity where verbal or any other mode of communication is not suitable. The importance of the study lies in two different aspects, firstly it provides a mathematical measure of human confidence from brain signal and applies it to multiple opinion fusion. From the viewpoint of information theory, the presented approach of analytical mechanics based information processing is entirely novel in the literature. The study also mathematically validates the use of Lagrangian as an analytical measure of confidence. Secondly in the context of collaborative decision making, the study successfully negates the idea of group decision averaging to obtain the final decision and also proves the efficacy of brain based communication over verbal or any other mode of communication.

XII. DECLARATION

Ethical Clearance of this study (Protocol No: ETCE/JU/21/AI01) is obtained from Hurip Independent Bioethics Committee having registration no ECR/103/Indt/WB/2013/RR-19.

REFERENCES

- [1] American Association for the Advancement of Science. *Monitoring Border Conflicts with Satellite Imagery: A Handbook for Practitioners*. URL: <https://www.aaas.org/resources/monitoring-border-conflicts-satellite-imagery-handbook-practitioners>.
- [2] Battista Biggio and Fabio Roli. "Wild patterns: Ten years after the rise of adversarial machine learning". In: *Pattern Recognition* 84 (2018), pp. 317–331.
- [3] Douglas Heaven. "Why deep-learning AIs are so easy to fool". In: *Nature* 574.7777 (2019), pp. 163–166.
- [4] Saugat Bhattacharyya et al. "Anytime Collaborative Brain-Computer Interfaces for Enhancing Group Decision-Making in Realistic Environments". In: (2020).
- [5] Jacobo Fernandez-Vargas et al. "Subject-and task-independent neural correlates and prediction of decision confidence in perceptual decision making". In: *Journal of Neural Engineering* (2021).
- [6] Behrooz Etesamipour and Robert J Hammell. "Aggregating Information Toward Military Decision Making". In: *2019 IEEE 17th International Conference on Software Engineering Research, Management and Applications (SERA)*. IEEE. 2019, pp. 19–26.
- [7] David P Williams, Michel Couillard, and Samantha Dugelay. "On human perception and automatic target recognition: Strategies for human-computer cooperation". In: *2014 22nd International Conference on Pattern Recognition*. IEEE. 2014, pp. 4690–4695.
- [8] Andreas Roeprtstorf, Geraint Rees, and Chris D Frith. "Optimally Interacting Minds". In: () .
- [9] Andrew J King et al. "Is the true ‘wisdom of the crowd’ to copy successful individuals?" In: *Biology Letters* 8.2 (2012), pp. 197–200.
- [10] Jonathan R Wolpaw et al. "Brain-computer interfaces for communication and control". In: *Clinical neurophysiology* 113.6 (2002), pp. 767–791.
- [11] Riccardo Poli, Davide Valeriani, and Caterina Cinel. "Collaborative brain-computer interface for aiding decision-making". In: *PloS one* 9.7 (2014), e102693.
- [12] Davide Valeriani, Caterina Cinel, and Riccardo Poli. "Group augmentation in realistic visual-search decisions via a hybrid brain-computer interface". In: *Scientific reports* 7.1 (2017), p. 7772.
- [13] Jonathan R Wolpaw. "Brain-computer interfaces as new brain output pathways". In: *The Journal of physiology* 579.3 (2007), pp. 613–619.
- [14] Christoph Guger et al. "How many people are able to control a P300-based brain-computer interface (BCI)?" In: *Neuroscience letters* 462.1 (2009), pp. 94–98.
- [15] Donnell J Creel. "The electrooculogram". In: *Handbook of clinical neurology*. Vol. 160. Elsevier, 2019, pp. 495–499.
- [16] Qiuiping A Wang. "Maximum entropy change and least action principle for nonequilibrium systems". In: *Astrophysics and Space Science* 305.3 (2006), pp. 273–281.
- [17] QA Wang et al. "Stochastic action principle and maximum entropy". In: *arXiv preprint arXiv:0704.0880* (2007).
- [18] A. Bar-Gill, P. Ben-Ezra, and I. Y. Bar-Itzhack. "Improvement of terrain-aided navigation via trajectory optimization". In: *IEEE Transactions on Control Systems Technology* 2.4 (1994), pp. 336–342.
- [19] R. Jiang et al. "Maximum entropy searching". In: *CAAI Transactions on Intelligence Technology* 4.1 (2019), pp. 1–8.
- [20] Sanjeeva Balasuriya, Nicholas T Ouellette, and Irina I Rypina. "Generalized Lagrangian coherent structures". In: *Physica D: Nonlinear Phenomena* 372 (2018), pp. 31–51.
- [21] Michal Branicki and Kenneth Uda. "Lagrangian uncertainty quantification and information inequalities for stochastic flows". In: *arXiv preprint arXiv:1905.08707* (2019).
- [22] Davide Valeriani, Riccardo Poli, and Caterina Cinel. "Enhancement of group perception via a collaborative brain-computer interface". In: *IEEE Transactions on Biomedical Engineering* 64.6 (2016), pp. 1238–1248.
- [23] Saugat Bhattacharyya et al. "Collaborative brain-computer interfaces to enhance group decisions in an outpost surveillance task". In: *2019 41st Annual International Conference of the IEEE Engineering in Medicine and Biology Society (EMBC)*. IEEE. 2019, pp. 3099–3102.
- [24] SR Soekadar et al. "Hybrid EEG/EOG-based brain/neural hand exoskeleton restores fully independent daily living activities after quadriplegia". In: *Science Robotics* 1.1 (2016), eaag3296–1.
- [25] Keum-Shik Hong and Muhammad Jawad Khan. "Hybrid brain-computer interface techniques for improved classification accuracy and increased number of commands: a review". In: *Frontiers in neurorobotics* 11 (2017), p. 35.
- [26] Jun Jiang et al. "Hybrid Brain-Computer Interface (BCI) based on the EEG and EOG signals". In: 24 (2014). 6, pp. 2919–2925. ISSN: 1878-3619. DOI: 10.3233/BME-141111.
- [27] B. Koo, Y. Nam, and S. Choi. "A hybrid EOG-P300 BCI with dual monitors". In: *2014 International Winter Workshop on Brain-Computer Interface (BCI)*. Feb. 2014, pp. 1–4. DOI: 10.1109/iwv-BCI.2014.6782566.
- [28] Blair S Williams. *Heuristics and biases in military decision making*. Tech. rep. ARMY COMBINED ARMS CENTER FORT LEAVENWORTH KS, 2010.
- [29] Yijun Wang and Tzyy-Ping Jung. "A collaborative brain-computer interface for improving human performance". In: *PloS one* 6.5 (2011), e20422.
- [30] Miguel P Eckstein et al. "Neural decoding of collective wisdom with multi-brain computing". In: *NeuroImage* 59.1 (2012), pp. 94–108.
- [31] Adrian Stoica. "Multimind: Multi-brain signal fusion to exceed the power of a single brain". In: *2012 Third International Conference on Emerging Security Technologies*. IEEE. 2012, pp. 94–98.
- [32] Ana Matran-Fernandez, Riccardo Poli, and Caterina Cinel. "Collaborative brain-computer interfaces for the automatic classification of images". In: *2013 6th International IEEE/EMBS Conference on Neural Engineering (NER)*. IEEE. 2013, pp. 1096–1099.
- [33] A Stoica et al. "Multi-brain fusion and applications to intelligence analysis". In: *Multisensor, Multisource Information Fusion: Architectures, Algorithms, and Applications 2013*. Vol. 8756. International Society for Optics and Photonics. 2013, 87560N.
- [34] Peng Yuan et al. "A collaborative brain-computer interface for accelerating human decision making". In: *International Conference on Universal Access in Human-Computer Interaction*. Springer. 2013, pp. 672–681.
- [35] Hubert Cecotti and Bertrand Rivet. "Subject combination and electrode selection in cooperative brain-computer interface based on event related potentials". In: *Brain sciences* 4.2 (2014), pp. 335–355.
- [36] Lei Jiang et al. "Rapid face recognition based on single-trial event-related potential detection over multiple brains". In: *2015 7th International IEEE/EMBS Conference on Neural Engineering (NER)*. IEEE. 2015, pp. 106–109.
- [37] Ana Matran-Fernandez and Riccardo Poli. "Brain-Computer Interfaces for Detection and Localization of Targets in Aerial Images". In: *IEEE Transactions on Biomedical Engineering* 64.4 (2016), pp. 959–969.
- [38] Davide Valeriani, Caterina Cinel, and Riccardo Poli. "Augmenting group performance in target-face recognition via collaborative brain-computer interfaces for surveillance applications". In: *2017 8th International IEEE/EMBS Conference on Neural Engineering (NER)*. IEEE. 2017, pp. 415–418.

- [39] Saugat Bhattacharyya et al. “Target Detection in Video Feeds with Selected Dyads and Groups Assisted by Collaborative Brain-Computer Interfaces”. In: *2019 9th International IEEE/EMBS Conference on Neural Engineering (NER)*. IEEE. 2019, pp. 159–162.
- [40] Davide Valeriani and Riccardo Poli. “Cyborg groups enhance face recognition in crowded environments”. In: *PLoS one* 14.3 (2019), e0212935.
- [41] Davide Valeriani, Riccardo Poli, and Caterina Cinel. “A collaborative Brain-Computer Interface to improve human performance in a visual search task”. In: *2015 7th International IEEE/EMBS Conference on Neural Engineering (NER)*. IEEE. 2015, pp. 218–223.
- [42] Riccardo Poli et al. “Towards cooperative brain-computer interfaces for space navigation”. In: *Proceedings of the 2013 international conference on Intelligent user interfaces*. 2013, pp. 149–160.
- [43] Davide Valeriani et al. “Augmenting group decision making accuracy in a realistic environment using collaborative brain-computer interfaces based on error-related potentials”. In: (2018).
- [44] Keith M Davis III et al. “Brainsourcing: Crowdsourcing Recognition Tasks via Collaborative Brain-Computer Interfacing”. In: *Proceedings of the 2020 CHI Conference on Human Factors in Computing Systems*. 2020, pp. 1–14.
- [45] Finda Dwi Putri. “A comparison study between different social interaction in multi-user Brain-Computer Interface (BCI) gaming: competitive vs. collaborative”. PhD thesis. University of Glasgow, 2020.
- [46] Vadim Grubov, Vladimir Maksimenko, and Vladimir Nedaivozov. “Development of the approach to collaborative BCI”. In: *2020 4th Scientific School on Dynamics of Complex Networks and their Application in Intellectual Robotics (DCNIR)*. IEEE. 2020, pp. 97–100.
- [47] Tien-Thong Nguyen Do and Thanh Tung Huynh. “Evaluate effects of multiple users in collaborative Brain-Computer Interfaces: A SSVEP study”. In: *bioRxiv* (2021).
- [48] Luis A Alexandre, Aurélio C Campilho, and Mohamed Kamel. “On combining classifiers using sum and product rules”. In: *Pattern Recognition Letters* 22.12 (2001), pp. 1283–1289.
- [49] Dymitr Ruta and Bogdan Gabrys. “Classifier selection for majority voting”. In: *Information fusion* 6.1 (2005), pp. 63–81.
- [50] Peter Emerson. “The original Borda count and partial voting”. In: *Social Choice and Welfare* 40.2 (2013), pp. 353–358.
- [51] Nikunj C Oza and Kagan Tumer. “Classifier ensembles: Select real-world applications”. In: *Information fusion* 9.1 (2008), pp. 4–20.
- [52] Giorgio Giacinto et al. “Intrusion detection in computer networks by a modular ensemble of one-class classifiers”. In: *Information Fusion* 9.1 (2008), pp. 69–82.
- [53] Boutheina A Fessi et al. “A clustering data fusion method for intrusion detection system”. In: *2011 IEEE 11th International Conference on Computer and Information Technology*. IEEE. 2011, pp. 539–545.
- [54] Tong Meng et al. “A survey on machine learning for data fusion”. In: *Information Fusion* 57 (2020), pp. 115–129.
- [55] Harald Ganster and Axel Pinz. “Active fusion using Dempster-Shafer theory of evidence”. In: *OEAGM/AAPR Workshop*. Citeseer. 1996, pp. 37–46.
- [56] Qi Chen et al. “Data classification using the Dempster-Shafer method”. In: *Journal of Experimental & Theoretical Artificial Intelligence* 26.4 (2014), pp. 493–517.
- [57] Francisco Javier Cabrerizo et al. “Analyzing consensus approaches in fuzzy group decision making: advantages and drawbacks”. In: *Soft Computing* 14.5 (2010), pp. 451–463.
- [58] Ignacio J Pérez et al. “On dynamic consensus processes in group decision making problems”. In: *Information Sciences* 459 (2018), pp. 20–35.
- [59] Maria José del Moral et al. “A comparative study on consensus measures in group decision making”. In: *International Journal of Intelligent Systems* 33.8 (2018), pp. 1624–1638.
- [60] Ignacio Javier Pérez et al. “A new consensus model for group decision making problems with non-homogeneous experts”. In: *IEEE Transactions on Systems, Man, and Cybernetics: Systems* 44.4 (2013), pp. 494–498.
- [61] Ignacio Javier Pérez, Francisco Javier Cabrerizo, and Enrique Herrera-Viedma. “A mobile decision support system for dynamic group decision-making problems”. In: *IEEE Transactions on Systems, Man, and Cybernetics-Part A: Systems and Humans* 40.6 (2010), pp. 1244–1256.
- [62] Mahima Gupta and BK Mohanty. “An algorithmic approach to group decision making problems under fuzzy and dynamic environment”. In: *Expert Systems with Applications* 55 (2016), pp. 118–132.
- [63] Zeshui Xu. “On multi-period multi-attribute decision making”. In: *Knowledge-Based Systems* 21.2 (2008), pp. 164–171.
- [64] Yong Zhang, Suhua Zhang, and Xiaomin Ji. “EEG-based classification of emotions using empirical mode decomposition and autoregressive model”. In: *Multimedia Tools and Applications* 77.20 (2018), pp. 26697–26710.
- [65] Geer Teng et al. “Design and development of human computer interface using electrooculogram with deep learninG”. In: *Artificial intelligence in medicine* 102 (2020), p. 101765.
- [66] Won-Du Chang. “Electrooculograms for Human–Computer Interaction: A Review”. In: *Sensors* 19.12 (2019), p. 2690.
- [67] Rolf Landauer. “The physical nature of information”. In: *Physics letters A* 217.4–5 (1996), pp. 188–193.
- [68] E. T. Jaynes. “Information Theory and Statistical Mechanics”. In: *Phys. Rev.* 106 (4 May 1957), pp. 620–630. DOI: 10.1103/PhysRev.106.620. URL: <https://link.aps.org/doi/10.1103/PhysRev.106.620>.
- [69] General Assembly of the World Medical Association et al. “World Medical Association Declaration of Helsinki: ethical principles for medical research involving human subjects”. In: *The Journal of the American College of Dentists* 81.3 (2014), p. 14.
- [70] Arnab Rakshit, Amit Konar, and Atulya K Nagar. “A hybrid brain-computer interface for closed-loop position control of a robot arm”. In: *IEEE/CAA Journal of Automatica Sinica* 7.5 (2020), pp. 1344–1360.
- [71] Antonio Maratea, Alfredo Petrosino, and Mario Manzo. “Adjusted F-measure and kernel scaling for imbalanced data learning”. In: *Information Sciences* 257 (2014), pp. 331–341.
- [72] Ivaylo Ivaylov, Milena Lazarova, and Agata Manolova. “EEG Classification for Motor Imagery Mental Tasks Using Wavelet Signal Denoising”. In: *2020 28th National Conference with International Participation (TELECOM)*. IEEE. 2020, pp. 53–56.
- [73] Nikhil Rathi, Rajesh Singla, and Sheela Tiwari. “Authentication framework for security application developed using a pictorial P300 speller”. In: *Brain-Computer Interfaces* 7.3–4 (2020), pp. 70–89.
- [74] Syed Kamran Haider et al. “Performance enhancement in P300 ERP single trial by machine learning adaptive denoising mechanism”. In: *IEEE Networking Letters* 1.1 (2018), pp. 26–29.
- [75] H Smith, R Gnanadesikan, and JB Hughes. “Multivariate analysis of variance (MANOVA)”. In: *Biometrics* 18.1 (1962), pp. 22–41.
- [76] Michael R Stoline. “The status of multiple comparisons: simultaneous estimation of all pairwise comparisons in one-way ANOVA designs”. In: *The American Statistician* 35.3 (1981), pp. 134–141.